Analysis of the trends in ambient methane in the Baltimore-Washington region and comparison to model output

Sayantan Sahu[1], Anna Karion[2], Israel Lopez-Coto[2], Xinrong Ren[3], Ross J. Salawitch[1,4,5], Russell R. Dickerson[1,4,5]

1. Department of Chemistry and Biochemistry, University of Maryland, College Park, Maryland, USA
2. National Institute of Standards and Technology, Gaithersburg, Maryland, USA
3. Air Resources Laboratory, National Oceanic and Atmospheric Administration, College Park, Maryland, USA
4. Department of Atmospheric and Oceanic Science, University of Maryland, College Park, Maryland, USA
5. Earth System Science Interdisciplinary Center, University of Maryland, College Park, Maryland, USA

Corresponding author: Sayantan Sahu (sayantan@umd.edu)

Key Points:

- Both versions of EDGAR (4.2 and 5.0) underestimate the regional anthropogenic emission of methane.
- The correlation of modeled versus measured methane was stronger with the EDGAR 5.0.
- Inclusion of fluxes of wetland emissions reduce the bias between modeled and measured methane, especially in summer at the rural site.

Abstract

We studied atmospheric methane observations from November 2016 to October 2017 from one rural and two urban towers in the Baltimore-Washington region (BWR). Methane observations at these three towers display distinct seasonal and diurnal cycles with maxima at night and in the early morning, reflecting local emissions and boundary layer dynamics. Peaks in winter concentrations and vertical gradients indicate strong local anthropogenic wintertime methane sources in urban regions. In contrast, our analysis shows larger local emissions in summer at the rural site, suggesting a dominant influence of wetland emissions. We compared observed enhancements (mole fractions above the 5th percentile) to simulated methane enhancements using the WRF-STILT model driven by two EDGAR inventories. When run with EDGAR 5.0, the low bias of modeled versus measured methane was greater (ratio of 1.9) than the bias found when using the EDGAR 4.2 emission inventory (ratio of 1.3). However, the correlation of modeled versus measured methane was stronger (~1.2 times higher) for EDGAR 5.0 compared to results found using EDGAR 4.2. In winter, the inclusion of wetland emissions using WETCHARTs had little impact on the mean bias, but during summer, the low bias for all hours using EDGAR 5.0 improved by from 63 to 23 nanomoles per mole of dry air or parts per billion (ppb) at the rural site. We conclude that both versions of EDGAR underestimate the regional anthropogenic emissions of methane, but version 5.0 has a more accurate spatial representation.

Plain Language Summary

In this study we analyzed methane observations from three towers in the Baltimore-Washington region and used these observations to evaluate anthropogenic and biogenic methane emission inventories. We found that anthropogenic methane sources dominate at the urban sites while wetland emissions dominate at the rural site. Significant discrepancies were observed between observations and methane outputs from a transport and dispersion model run with different inventories, indicating substantially underestimated methane emissions in these inventories. The low bias was greater with a newer version (EDGAR 5.0) than with an older version (EDGAR 4.2), however the correlation was stronger with the newer version. We attribute the stronger correlation to improved spatial distribution of methane emissions within the newer version. Adding wetland emissions reduced bias and improved the seasonal cycle in modeled methane at the rural site.

1. Introduction

Methane is an important and not yet fully understood greenhouse gas, with a global warming potential of about 80 times more than carbon dioxide over a 20 year time horizon (Sixth Assessment Report — IPCC), although with an atmospheric lifetime much shorter than carbon dioxide. There are both natural and anthropogenic sources of methane. For example, natural sources include wetlands and wild animals while anthropogenic sources include the production, transmission, distribution, and use of natural gas, as well as coal, livestock, wastewater treatment, and landfills. In the United States (U.S.), natural gas and petroleum systems are the second largest source of methane emissions after agriculture (Inventory of U.S. Greenhouse Gas Emissions and Sinks | U.S. EPA). Urban areas are a significant source of anthropogenic methane emissions, often dominated by fugitive emissions from the natural gas distribution and usage (Ren et al., 2018; Plant et al., 2019; Sargent et al., 2021).

Methane emissions from urban areas remain uncertain. Studies have attempted to assess and quantify the methane emissions from natural gas leakage in urban centers and the transmission and storage (T&S) sector as a whole (Alvarez et al., 2012, 2018; Peischl et al., 2013; Phillips et al., 2013; Jackson et al., 2014; Gallagher et al., 2015; Kathryn et al., 2015; Lamb et al., 2015; Zimmerle et al., 2015; Hendrick et al., 2016; Cambaliza et al., 2017). Substantial disparities exist between bottom-up estimates (inventories) and top-down estimates (based on atmospheric measurements) with top-down estimates generally much larger than bottom-up values (Lamb et al., 2016; Turner et al., 2016; Ren et al., 2018; Lopez-Coto et al., 2020). A recent study by Plant et al., (2019) used aircraft measurements to conclude that methane emissions from many urban centers along the U.S. East Coast are more than twice those in inventories. Ren et al., (2018) and Lopez-Coto et al., (2020) used airborne measurements to determine that the winter (February) methane emission rates in 2016 in the Baltimore-Washington region (BWR) were 2.7 to 2.8 times the US national greenhouse gas inventory for 2012. Huang et al., (2019), used atmospheric inversions with methane observations from towers in the BWR and found methane emissions underestimated by the existing inventories in fall, winter, and spring but overestimated in summer because of excess modeled wetland emissions.

Few studies have looked at how models reproduce observed diurnal and seasonal trends of methane. Yadav et al., (2019) and He et al., (2019) used continuous observations (tower-based and remote-sensing, respectively) in the Southern California air basin to show seasonality in urban methane emissions. Sargent et al., (2021) showed distinct seasonality in methane emissions in Boston using in-situ observations in that city as well. Huang et al., (2019) used data from afternoon hours (12 pm to 5 pm) and discovered a significant seasonality in urban methane emissions in the BWR. The objective of our study is to evaluate anthropogenic and biogenic methane emission inventories with ambient observations from towers. The aim is to better understand the sources and to evaluate existing inventories of methane. We studied in-situ methane data from the BWR under the Northeast Corridor (NEC) project using two urban towers ARL (Arlington, VA), NEB (Northeast Baltimore, MD), and one rural tower, BUC (Bucktown, MD) (Karion et al., 2020). Karion et al., (2020) discussed methane measurements from two of these three towers – ARL and BUC. The methane observations from these towers displayed distinct seasonal and diurnal cycles with seasonal maxima in winter at the urban towers reflecting greater emissions and reduced vertical mixing, and larger vertical gradients at night and early morning, indicating significant local emissions and higher concentrations when the planetary boundary layer (PBL) is shallow. At BUC, the rural site, Karion et al., (2020) observed large vertical gradients during the early morning hours in the summer, suggesting substantial local wetland emissions expected to peak when the surface is warm. In our study, we compared modeled methane enhancements to observed enhancements. We used the meteorological WRF (Weather Research and Forecasting) Model (Skamarock et al., 2008) in combination with Lagrangian dispersion model STILT (Stochastic Time-Inverted Lagrangian Transport model) (Lin et al., 2003; Nehrkorn et al., 2010) to simulate time series of methane at each tower location. We compared the tower methane observations with the model outputs and used the ambient observations to evaluate the anthropogenic and biogenic methane emission inventories.

2. Methods

2.1. Tower locations and observations

The NEC tower network, currently consisting of 29 stations, was initiated in 2015, with the primary objective to better quantify urban emissions of anthropogenic greenhouse gases (Karion et al., 2020). Sixteen stations were established around the BWR to estimate greenhouse gas emissions using inverse modeling techniques (Lopez-Coto et al., 2017; Mueller et al., 2018). The tower network design and location under NEC, data collection, processing, instrumentation, and calibration have been discussed in detail in earlier publications (Welp et al., 2013; Verhulst et al., 2017; Lopez-Coto et al., 2017; Mueller et al., 2018; Karion et al., 2020). We used continuous, hourly measurements of methane from the three towers in the region - NEB, ARL, and BUC. NEB is located in the city of Baltimore, where the median household income is $52,164, while ARL is in Arlington, VA, a moderately developed suburb of Washington DC with over twice the median income of Baltimore ($122,604) (U.S. Census Bureau). Both are classified as urban towers (Karion et al., 2020). BUC is located in Bucktown, MD, on the eastern side of Chesapeake Bay, in a wetland-dominant region (Karion et al., 2020). The location of these towers and the sampling heights are provided in Table S1 & Figure S1, and also in Huang et al., (2019) and Karion et al., (2020).

We analyzed the diurnal and seasonal variation of methane at these three towers using contour plots as previously done in Bloomer et al. (2010). We computed the hourly averages of the methane observations for each month to generate these plots. We used data for the period November 2016 to October 2017 and focused our model comparison analysis in two ecological seasons - winter (December 2016 to February 2017) and summer (June to August 2017). Our research considered data from the entire diurnal cycle to determine how effectively the model run with various inventories can replicate the observed diurnal trends. We used results from only the lower sampling height (46m to 50 m above ground level) for the model bias comparison but obtained similar results when considering data from the upper sampling height. Data from both sampling heights of each tower were used for the vertical gradient analysis.

2.2. Description of model and inventories

Our study used the STILT transport and dispersion model (Lin et al., 2003b) run with meteorological data from WRF model (Skamarock and Klemp, 2008; Skamarock et al., 2008) and configured as described in (Karion et al., 2021). STILT was run 120 h backward in time from the observation points – the locations of the towers in our study. The surface influence (proportional to the residence time of a particle over a given pixel and within the planetary boundary layer) for each observation, or footprint, was calculated. The surface influence at each pixel was multiplied by the emissions inventory's surface flux (μmol/m^2/s). The sum over all pixels equals the modeled mole fraction enhancement at the tower site. Footprints were generated for each tower for a regional domain (bounds 92.0 W, 68.0 W, 33.0 N, 47.0 N) at 0.1-degree resolution. The domain is shown in Figure S2.

We used two anthropogenic CH_4 emission inventories – the Emission Database for Global Atmospheric Research versions 4.2 (hereafter referred to as EDGAR 4.2) (Janssens-Maenhout et al., 2013) and 5.0 (hereafter referred to as EDGAR 5.0) (EDGAR - Joint Research Centre Data Catalogue - EDGAR v5.0 Greenhouse Gas Emissions - European Commission; Crippa et al., 2019) for 2012. The inventories have a horizontal resolution of 0.1° latitude by 0.1° longitude. There is no seasonality in methane emissions in EDGAR 4.2 and essentially no variation (< 5%) with season in EDGAR 5.0 in our model domain or near our towers. Here, we used the annual average of emissions for a particular year in the model. We chose these two versions of EDGAR because they have the most different spatial representation of emissions, with EDGAR 4.2 placing more emissions in urban centers (i.e., emissions are downscaled via population) than EDGAR 5.0. (Janssens-Maenhout et al., 2013). The distribution of methane emissions within the inventories for the area near the towers is discussed in the results section.

2.3. Comparison of observations and model outputs

Our study considered several methods to compare modeled wetland emissions with observations. To account for wetland methane emissions, we used wetland fluxes derived from WetCHARTs, with a horizontal resolution of 0.5° latitude by 0.5° longitude (Bloom et al., 2017). WetCHARTs consists of 18 emission models, of which nine exhibit higher magnitude of methane wetland fluxes than others, while the remaining 9 models are significantly lower in magnitude and have different spatial allocations of wetland emissions (Figures S3a-b). We calculated the mean from the 9 models with higher magnitude (hereafter referred to as 'wet 3a') and lower magnitude (hereafter referred to as 'wet 4a') of wetland fluxes averaged monthly over 15 years. We also determined the mean of all 18 models over 15 years (hereafter referred to as 'wet ma') for comparison with observations. In addition to the three scenarios mentioned above (wet 3a, wet 4a and wet ma), we have downscaled the emissions to our 0.1° model resolution using the wetland fraction (calculated as the sum of woody and herbaceous wetlands) from the National Land Cover Database (NLCD) 2016 (Yang et al., 2018), conserving the mass within each 0.5° cell. We have referred to the scenarios as 'wet 3b', 'wet4b', and 'wet mb'.

We adopted a simple approach to directly compare the model outputs with methane tower observations. The WRF-STILT model footprints are convolved (multiplied pixel by pixel and then summed) with inventories (both anthropogenic and WetCHARTs) to simulate methane mole fraction enhancement in nanomoles of methane per mole of dry air, (nmol mol^{-1}), or parts per billion (ppb), interpreted as excess methane over the atmospheric background concentration. Due to the small number of towers used in this work and the fact that none of them could really be considered a background tower, we decided to apply a simplified background methodology, treating each tower independently, as opposed to more complex background methods as described in Karion et al., (2021). We subtracted the 5th percentile, similarly to Pak et al., (2021) but determined seasonally for each tower, from the absolute methane mole fractions from both the tower observations and the modeled output. We repeated our analysis with the 2nd, 10th, and 15th percentile (Tables S2-3) subtracted from the methane tower observations and the model results and found that while the choice of percentile impacts the magnitude of the biases it did not impact the direction of the biases, the normalized mean bias (see below), nor the general conclusions; here, we presented results using the 5th percentile.

We added the WetCHARTs modeled outputs to the EDGAR outputs (and subsequently deducted the 5th percentile) to determine if the inclusion of wetland emissions could bring better agreement between the model and observations. We used the bias and normalized mean bias (hereafter referred to as NMB) of methane to quantify the discrepancies between the model and observations. The NMB gives a good idea of how significant the bias is relative to the signal (enhancement). The two quantities were calculated as follows,

$$\text{Mean bias (ppb methane)} = \frac{\sum_{i=1}^{n}(\text{model}_i - \text{obs}_i)}{n}$$

(Eq. 1)

$$\text{Normalized mean bias (NMB)} = \frac{\sum_{i=1}^{n}(\text{model}_i - \text{obs}_i)}{\sum_{i=1}^{n}\text{obs}_i}$$

(Eq. 2)

(n = number of observations)

Here, 'obs' and 'model' refer to the observations and modeled output above the 5th percentile. A negative mean bias will be reflective of the model underestimating observations. We also calculated the least squares coefficient of determination (r^2) between methane observations and the model.

We investigated the methane vertical gradients between the two inlet heights at the three towers and compared these with model output. The analysis of vertical gradients will help understand whether the towers are located in the vicinity of sources (Monteiro et al., 2022). When the PBL is not well-mixed (e.g., at night or early morning), ground-level emissions near the tower result in higher concentrations at the lower level, thus larger gradients indicate higher emissions near the tower.

3. Results

3.1. Analysis of methane observations at the three towers

Methane measurements from the three towers in our study display distinct diurnal and seasonal cycles with daily maxima in the early morning and night hours (Figure 1). The presence of such distinct early morning and nighttime local maxima indicates local emissions. These maxima can be explained by the buildup from local emissions in the shallower boundary layer that are later dissipated due to turbulent mixing in the afternoon hours. The methane contour plots at the urban sites, NEB and ARL, show that this early morning enhancement is greatest during winter, but a secondary maximum in the early morning also appears in the late summer months (around August). The higher ambient concentration in the early morning and night hours in winter can be attributed to both enhanced anthropogenic methane emissions in winter and to the seasonality of boundary layer heights (Huang et al., 2019; Karion et al., 2020). Minima are observed in the summer afternoons when the PBL is deepest. The pattern indicates the importance of local emissions in the vicinity of the tower. The urban sites show a dominant winter peak suggesting that leakage from the natural gas (NG) system may be a major local source, if NG system emissions are higher in winter than summer, as suggested by previous urban studies (He et al., 2019; Sargent et al., 2021). The secondary summer peak indicates that other, likely biogenic, sources may also be at play. Seasonality in meteorological conditions, including the PBL, also plays a role.

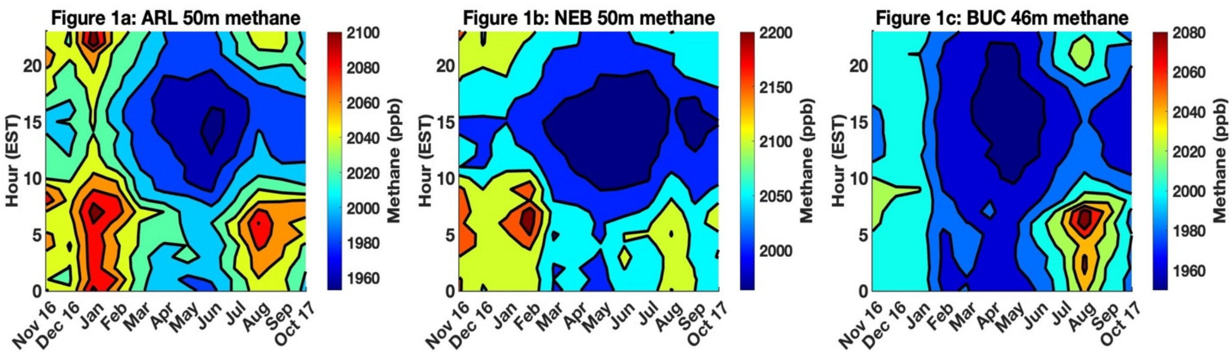

Figure 1. Methane contour plots showing diurnal and seasonal variation of methane at the three towers for the period November 2016 – October 2017. The data are from the lower inlet height of the towers 50 m above ground level for NEB and ARL and 46 m for BUC. Note the color bars are different in each plot.

Unlike the urban sites, the rural BUC site shows a dominant early morning enhancement during the summer months, indicating a strong local biogenic process more pronounced at higher temperatures. This late summer maximum is coincident with the summer maxima discussed for the urban towers (ARL and NEB), indicating that these towers might also be impacted by biogenic sources. BUC is located in Dorchester County, MD, with close to 68,400 hectares of estuarine and palustrine wetlands, besides agricultural land. This site shows a minor winter maximum likely related to PBL dynamics coupled with some minor emissions in winter. The absolute values of the methane mole fractions are greatest at NEB and smallest at BUC. These patterns suggest that urban methane emissions are greater than rural emissions in the BWR.

3.2. Comparison of observed and modeled diurnal cycles of methane

We analyzed both the observed and modeled diurnal variations of methane enhancements at all three towers to investigate how accurately the models captured the observed diurnal trends of methane. The modeled outputs were derived from the WRF-STILT runs with the EDGAR inventories as described in the Methods section. The plots in Figures 2a-f show the observed diurnal cycles of methane enhancements plotted along with the WRF-STILT model predicted diurnal cycles, run with EDGAR 4.2 or EDGAR 5.0.

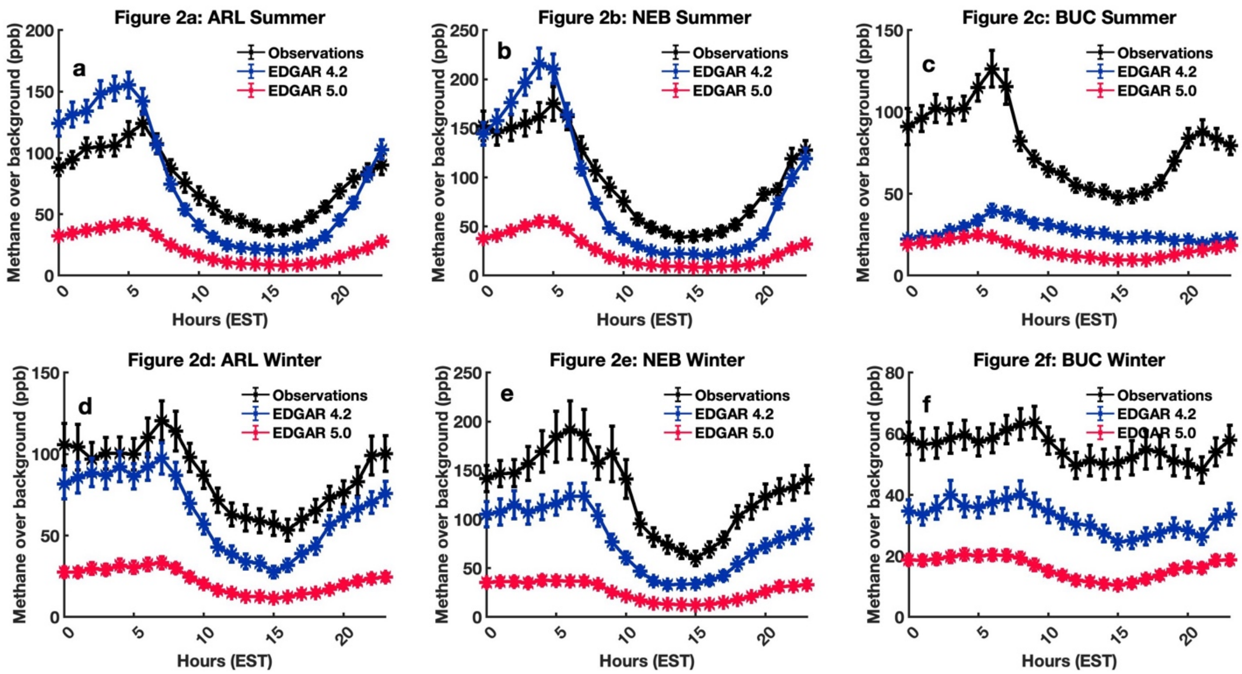

Figure 2. Diurnal cycles of methane enhancements during summer (a-c) and winter months (d-f) at two urban towers, ARL and NEB, and one rural tower, BUC. The black line represents the hourly averaged methane observations; the blue and red lines represent modeled diurnal trends run with EDGAR 4.2 and EDGAR 5.0 inventories respectively using the 5th percentile as background. The error bars represent the standard error of the mean, i.e., the standard deviation of the hourly observations divided by the square root of the number of observations used to calculate the mean.

3.2.1. Analysis of observed diurnal cycles of methane

The observed diurnal cycles of methane enhancements for the three sites displayed a pronounced maximum in the early morning and the night, as also shown in Figure 1 and suggesting local emissions. As explained earlier, local emissions produce maxima in concentrations when the PBL is shallow. At the two urban sites, the magnitude of observed early morning maximum was greater during the winter than the summer. A plausible reason could be greater local anthropogenic methane emissions during winter due to increased NG use for heating, resulting in a higher early morning maximum in the diurnal cycle (He et al., 2019; Sargent et al., 2021), but also possibly caused by lower mixing layer depths in winter compared to summer. At BUC, a prominent diurnal cycle was seen during summer with a weaker variation during winter, suggesting that it is influenced by strong summer-time local sources, while winter-time enhancements originated farther from the tower, or by weak, local sources. Figure 1b shows evidence of strong seasonal emissions, likely from wetlands, at BUC that may explain the diurnal cycle in summer and near absence of it in winter.

3.2.2. Analysis of modeled diurnal cycles of methane to determine model - observation bias

It is evident from Figures 2a-f that significant discrepancies exist between the modeled and observed enhancements at all three towers. The WRF-STILT runs with both EDGAR inventories underestimate the enhancement of methane substantially in most cases at all three sites. EDGAR does not include wetland emissions of methane, which can plausibly explain the discrepancies between model and methane observations, especially in summer. WRF-STILT driven with the EDGAR 5.0 inventory has a greater negative bias relative to methane observations than when driven with EDGAR 4.2. In general, the EDGAR 4.2 inventory appears to reproduce the observed diurnal trend better (with less bias) than EDGAR 5.0.

In the winter, both EDGAR inventories underestimate methane during all hours, at all three towers. This is clear evidence of the model underestimating anthropogenic methane emissions, as we do not expect large natural emissions from wetlands in winter. The bias is greater with EDGAR 5.0 than with EDGAR 4.2, however. The spatial distributions of methane emissions within the area near the towers for both EDGAR 4.2 and EDGAR 5.0 are shown in Figures 3a-b. The total methane emissions within this area are significantly higher in EDGAR 4.2 (a factor of 1.85 in the area shown in Figure 3) compared to EDGAR 5.0. In addition, EDGAR 4.2 has more concentrated emissions around the cities, which strongly influence observations at the urban sites. These factors combined result in higher modeled enhancements relative to EDGAR 5.0 and thus lower bias. Both EDGAR inventories underestimate observed methane enhancements at BUC during winter, when wetland emissions are minimal, suggesting that these inventories also underestimate anthropogenic methane emissions upwind of this rural site. The bias is lower, in absolute magnitude, during the afternoon hours, when the boundary layer is well mixed, than at other times of the day, but still substantial.

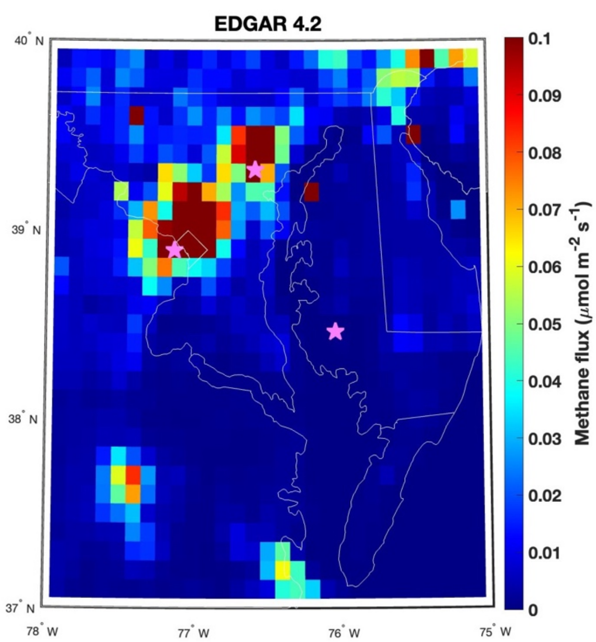

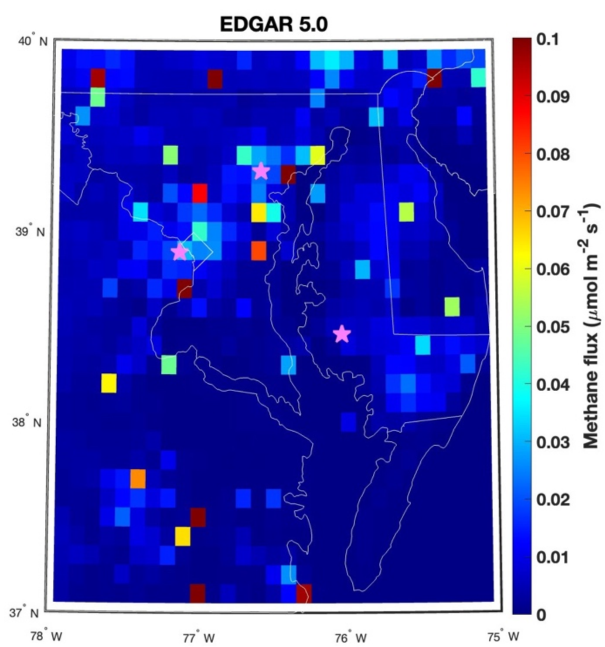

Figure 3a **Figure 3b**

Figures 3. Distribution of CH_4 emission fluxes (in units of μmol/m^2/s) in EDGAR 4.2 (left) and EDGAR 5.0 (right) around the towers used in our analysis. The pink stars represent the towers in our study. Color axis has been truncated for clarity.

At the urban towers during the summer months, EDGAR 5.0 underestimates methane observed enhancements at all hours. However, EDGAR 4.2 underestimates methane enhancements during afternoon hours but overestimates them during early morning hours. A plausible explanation of the overestimation could be lower emissions of methane during summer compared to winter (Huang et al., 2019), combined with potential inaccurate representation of planetary boundary layer dynamics in the transport model. Emissions of methane within EDGAR versions used here are averaged annually, so there is no temporal variability in the anthropogenic emissions used in the model. During the summer months at BUC, the rural site in an area of extensive estuaries and other wetlands, significant discrepancies between the modeled and observed enhancements exist at all hours. This can be explained by the fact that EDGAR inventories do not include natural (wetland) emissions, discussed below.

3.2.3. Mean bias, NMB, correlation between observed and modeled methane enhancements

To quantify the bias between model outputs and observed methane enhancements, we analyzed the mean bias (Eq. 1), normalized mean bias (NMB, Eq. 2), and the coefficient of determination (r^2). The results for summer and winter afternoon hours (12 pm to 3 pm EST) are tabulated in Table 1 and all hours in Table S4.

Table 1

Mean bias (in ppb of methane, i.e., nmol/mol), normalized mean bias, and r^2 between modeled and observed enhancements for winter and summer afternoon hours, using the 5th percentile background.

Tower	Inventory	Season	Mean bias (ppb)	NMB	r^2
BUC	EDGAR 4.2	winter	-22.26	-0.44	0.26
NEB		winter	-42.50	-0.52	0.38
ARL		winter	-26.97	-0.40	0.33
BUC	EDGAR 5.0	winter	-37.50	-0.74	0.29
NEB		winter	-65.93	-0.80	0.39
ARL		winter	-51.78	-0.77	0.36
BUC	EDGAR 4.2	summer	-35.10	-0.60	0.30
NEB		summer	-26.98	-0.49	0.18
ARL		summer	-18.78	-0.39	0.28
BUC		summer	-46.38	-0.80	0.36

NEB	EDGAR 5.0	summer	-43.39	-0.79	0.22
ARL		summer	-36.40	-0.75	0.36

Note. The corresponding table for all hours is in Table S4.

On average, the modeled methane enhancements are biased low in winter by approximately 22 ppb to 37 ppb at BUC, and by 27 ppb to 66 ppb for the urban towers (NEB and ARL), depending on which EDGAR inventory is used. The bias is greater for the urban towers compared with the rural site, and greater with EDGAR 5.0 than with 4.2 at all sites. During summer, the low bias ranges from approximately 19 ppb to 46 ppb when considering the three towers. There is a greater low bias at the urban towers (NEB and ARL) during winter than at BUC. Conversely during summer, the model low bias was greater at BUC than at the two urban towers. We attribute these tendencies to weak wetland emissions during winter at the rural site that are amplified during summer. The urban towers are influenced by the local anthropogenic methane emissions, likely from the NG distribution system or end usage, which recent studies have suggested are higher in winter (He et al., 2019; Huang et al., 2019; Sargent et al., 2021). Moreover, during winter, local emissions have a greater impact on observed enhancements due to the shallower boundary layer. We arrive at the same conclusions when considering all hours of the day (Table S4). The low bias is reduced to 1 ppb to 10 ppb of methane at the urban towers during summer when using EDGAR 4.2 due to the overestimation by the model at early morning hours (Figures 2a-b). The bias is the smallest when only afternoon hours are considered, possibly due to the smaller overall enhancements and because the transport model may perform better under well-mixed conditions.

We compare the coefficient of determination (r^2) between modeled and observed CH_4 enhancements within each season. Modeled methane from EDGAR 5.0 correlates better with observations than EDGAR 4.2 in most cases despite the greater low bias, likely due to the improved spatial distribution of methane emissions in the newer version. However, while EDGAR 5.0 correlates better with observations, it has a greater negative bias because it has lower emissions, especially around urban centers. We note here that although a newer version of EDGAR (6.0) is now available, it is very similar in both magnitude and spatial distribution to EDGAR 5.0 (Figure S4), so we would not expect its use to yield any significant difference in our results.

3.3. Incorporating wetland emissions using WETCHARTs

The summer concentration peak at BUC (an area of extensive estuaries and other wetlands) suggests strong natural flux from wetlands, which are not included in the EDGAR anthropogenic emissions inventory. We thus ran the model with WetCHARTs version 1.3.1 and added the resulting modeled enhancements from wetland emissions to the anthropogenic enhancements from EDGAR 5.0 (See Figure 4, S5a-b and Tables S7-10). We used WRF-STILT outputs with EDGAR 5.0 rather than 4.2 as EDGAR 5.0 better correlated with observations. Our findings suggest that during winter, the addition of various WetCHARTs combinations has little impact on the bias, as expected (wetland emissions are very small in winter (Figure S3)). The combinations 'wet 3a' and 'wet 3b' produce the smallest bias under all scenarios, as these include the WetCHARTs members that have significantly higher methane flux than others. During winter afternoon hours, the model was still biased low by approximately 35 ppb, 63 ppb, 50 ppb at BUC, NEB, and ARL, respectively. The continued underestimation by the model during winter after incorporating wetland emissions is clear evidence of EDGAR 5.0 underestimating anthropogenic emissions of methane in this region.

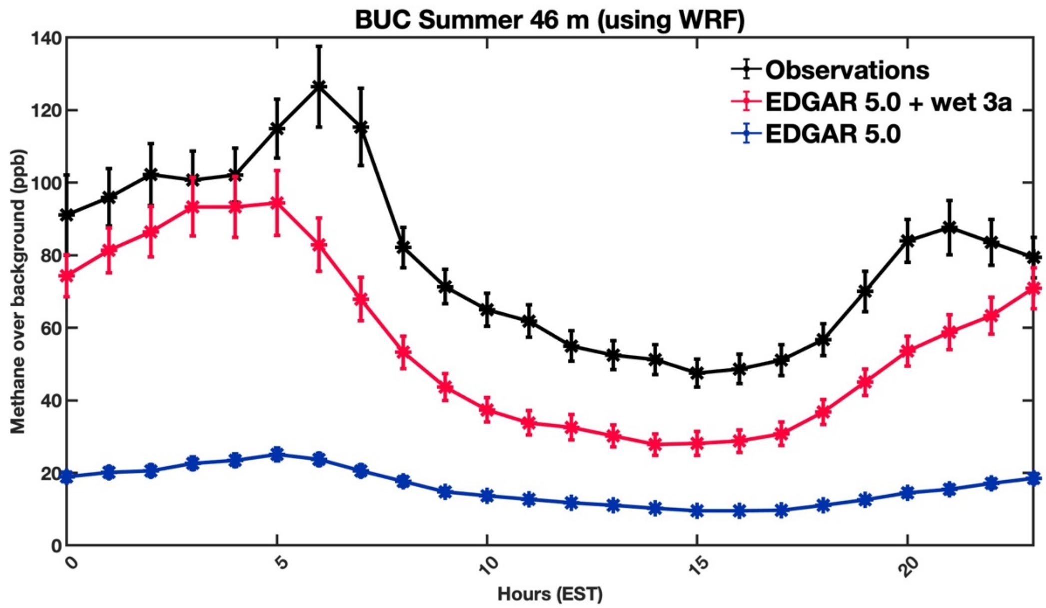

Figure 4: Diurnal cycle of methane at BUC during summer. The black line represents the hourly averaged methane observations. The red and blue lines represent the model predicted diurnal trends using the EDGAR 5.0 inventory, with and without wetland emissions, respectively. The error bars represent the standard error of the mean of the data in hourly bins.

In summer, we observe much better agreement between modeled and observed CH_4 enhancements after including the effect of wetland emissions in the model. The negative model bias falls to approximately 20 ppb during afternoon hours at the three towers and ranges from approximately 12 to 28 ppb when considering all hours. Thus, even after adding wetland emissions in summer, a substantial bias remains, suggesting that WetCHARTs either underestimates the magnitude of wetland emissions or that the anthropogenic underestimation is so large that it is not compensated for by including wetland emissions. Adding WetCHARTs improves the seasonal cycle in modeled CH_4 at BUC as the summer afternoon low bias improves from approximately 46 ppb to 20 ppb. We compare the correlation (Tables S7-10) for the summer and winter seasons after adding modeled methane enhancements from WetCHARTs and find no improvement. The above observations show that WetCHARTs can be improved in both magnitude and spatial allocation of wetland emissions of methane.

3.4. Analysis of observed and modeled Vertical gradient of methane

We compared the observed and modeled vertical gradient of methane at the three towers for the winter and summer months. The vertical gradient was calculated as the difference in methane observations between the lower and the upper height, divided by the difference in inlet heights. A weak vertical gradient is indicative of a better mixed boundary layer or absence of strong local sources and sinks. When the boundary layer is not well-mixed, the gradient shows if there are local sources. The vertical gradient can help us better understand if strong local sources of methane influence the tower observations (Wyngaard et al., 1984; Dyer, 1974; Patton, Sullivan and Davis, 2003; Monteiro et al., 2022). However, the difference between modeled and observed vertical gradients is a function of both the accuracy of the emissions used in the model and the ability of the transport and dispersion model to simulate vertical mixing accurately. Figure 5 shows the diurnal variations of the observed and modeled vertical gradients at the three towers in summer (Figures 5a-c) and winter (Figures 5d-f).

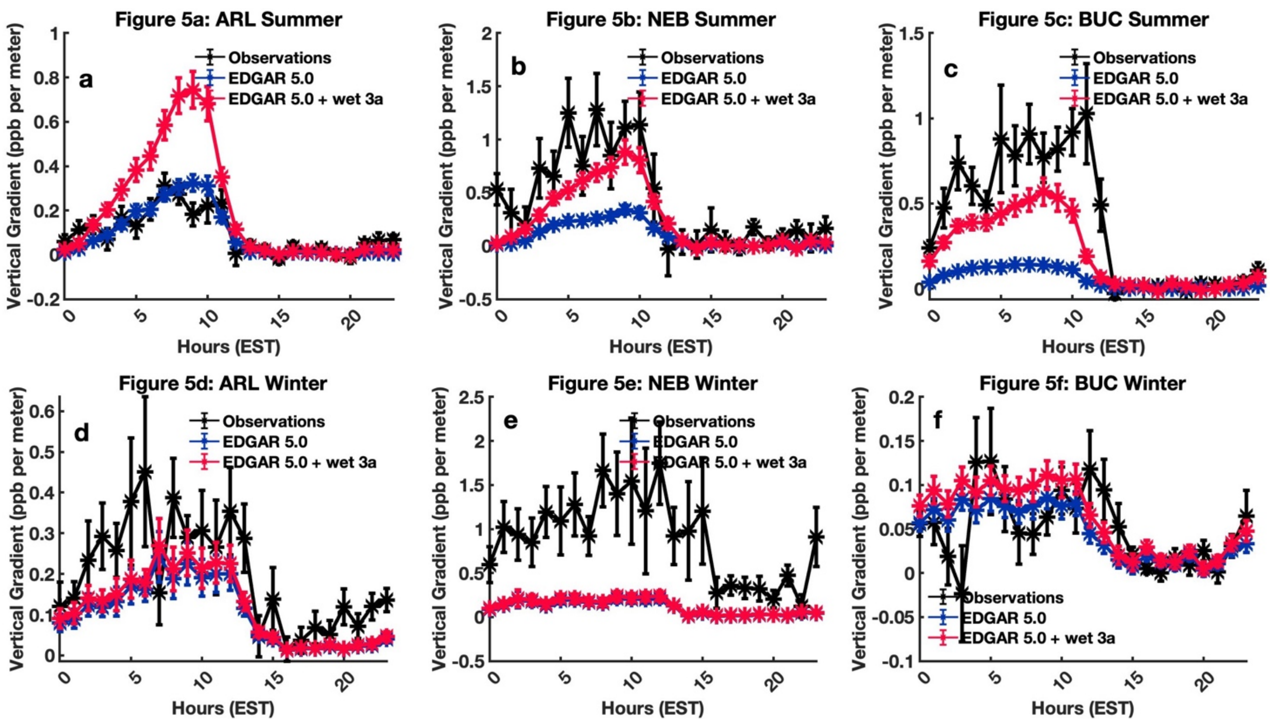

Figure 5. Vertical gradients of methane at the three towers in summer (a-c) and in winter (d-f). The black lines represent observed vertical gradient between the two inlet heights at the towers. The blue and the red lines represent the model simulated vertical gradient without wetland emissions and with 'wet 3a' emissions from WetCHARTs, respectively. The error bars represent the standard error of mean of vertical gradients in hourly bins.

3.4.1. Observed Vertical gradient of methane

We observe a large vertical gradient at both urban towers in the early morning hours that plummets in the afternoon hours (consistent with the early morning concentration maximum seen in Figure 1). The strong vertical gradient in the morning hours indicates that the towers are situated in the vicinity of methane sources. The pattern is similar during winter and summer; however, the morning vertical gradient is slightly higher during winter, which can be attributed either to the seasonality of the nocturnal vertical mixing or greater anthropogenic methane emissions during winter or both. In contrast, at BUC, we observe strong vertical gradients during summer, but they are close to zero during winter indicating that local sources during this season are very weak. The strong summer vertical gradients can be explained by local wetland emissions influencing observations at this site, and the bulk of anthropogenic sources being farther away.

3.4.2. Modeled Vertical gradient of methane

We analyzed how reliably WRF-STILT run with EDGAR 5.0 can reproduce the observed vertical gradients at the three towers. We included modeled methane enhancements from WetCHARTs "3a" (the mean of the high-emission members) to account for biogenic emissions, because the "3a" version better matched summer observations at BUC in our previous analysis. The discrepancy between observed and modeled vertical gradients at all three sites is lowest during the late afternoon hours when the boundary layer is well-mixed. The results are congruent with the results in the previous section, where we compared the observed and model-simulated diurnal patterns of methane enhancements. At NEB and ARL, the inclusion of wetland emissions during winter does not substantially improve the model bias, as they are very small in winter (see Tables S7-8). At ARL, during winter, we observed good agreement between model outputs and observations, with a bias of approximately 0.1 ppb per meter during early morning hours and less than 0.1 ppb per meter during the afternoon. At NEB, the model was biased low by approximately 1 ppb per meter in the early morning hours and approximately 0.2 ppb per meter during the afternoon hours, most likely due to local sources being underestimated in EDGAR 5.0.

During summer, at ARL, the model run with EDGAR 5.0 reproduces the observed diurnal trend in vertical gradient remarkably well; however, the inclusion of wetland emissions overestimates the early morning gradient. In contrast, at NEB during summer, the model simulations with the addition of wetland emissions significantly reduce the bias between the modeled and observed vertical gradient, from approximately 1 to 0.2 ppb per meter. Thus, either wetland emissions are influencing observations at NEB in summer, or (more likely, given the lack of nearby wetlands) the additional modeled emissions are compensating for the large under-estimation of anthropogenic emissions in EDGAR 5.0 at this site. At BUC, during winter, in the absence of any strong local sources, we observe good agreement between model outputs and observations at all hours. During summer, when wetland emissions are greatest, the addition of WetCHARTs output in the model significantly reduces the bias, especially during morning hours, when local emissions are most significant.

3.5. Contrasting urban sites - NEB and ARL

When we compare the methane diurnal cycle at the two urban towers, we find greater methane enhancements at NEB when compared to ARL. The absolute methane mole fractions are also greater at NEB than ARL (Figures 1a-b). This may be the result of ARL being generally more upwind of the BWR and NEB being more generally downwind, or to greater emissions near NEB, possibly due to fugitive methane emissions from leaks in the delivery system (Weller, Hamburg and von Fischer, 2020). In this paper, we have pointed out the potential impact of natural gas on observations, but local sources could also be from urban wastewater treatment and landfills.

Demographics and infrastructure may play a role in the differences of methane concentrations at the two sites. The observation raises a pertinent question of environmental justice (Weller et al., 2022), as methane concentrations may correlate with higher concentrations of other pollutants that affect health outcomes; future studies should further investigate differences in methane sources and emissions magnitudes in these two cites (Arlington, VA and Baltimore, MD). When comparing observations to modeled enhancements, we discover more extreme bias toward low values in the model for the NEB than ARL (NMB 0.80 vs 0.77 for winter afternoon with EDGAR 5.0), see Table 1. The difference can be because EDGAR 5.0 emissions are too low near NEB but more accurate near ARL, compared to observed data, as also suggested by the vertical gradients.

5. Conclusions

Our study compared methane observations from three towers with output from a Lagrangian model using diurnal patterns and vertical gradients. Results suggest that anthropogenic methane emissions dominate in the urban areas (sites NEB and ARL) while natural (i.e., wetland) sources dominate at the rural site (BUC). Significant discrepancies were found between models driven by EDGAR and observations; while EDGAR 5.0 seems to have an improved spatial distribution of emissions (as suggested by higher correlations with observed enhancements), its emissions magnitude in these two cities is too low. EDGAR 4.2, with larger urban emissions, compared more favorably with observations in terms of magnitude. Both daily cycle and vertical gradient comparisons point toward higher local emissions near NEB relative to ARL and higher emissions during winter than in summer at these urban sites, although more work is needed to confidently conclude this. In addition, adding wetland emissions from WetCHARTs significantly improved the agreement between modeled and observed vertical gradients especially in summer at BUC. While adding wetland emissions from WetCHARTs reduced discrepancies in terms of bias, especially in summer, the lower correlation observed might indicate that the distribution of these emissions could still be improved and that we need better wetland models with greater resolution to replicate observations from the mid-Atlantic wetland region. Besides the known anthropogenic emissions, we found evidence of additional summer (possibly biogenic) emissions at the urban sites based upon analyses of the seasonal and temporal patters of observed methane. Future studies should investigate the source of summertime emissions around these sites and the strength of these sources relative to the anthropogenic source of methane. We note that here we have investigated CH_4 observations near towers using a simple seasonal background; a more quantitative determination of CH_4 emissions would require a more sophisticated treatment of background (e.g., Karion et al., 2021) and likely a higher resolution modeling framework. Finally, future measurements of ethane and ^{13}C isotopic analysis along with methane might help distinguish the relative strength of biogenic and anthropogenic sources.

Acknowledgments and Data Availability

The authors thank Anthony Bloom (JPL) for providing the WetCHARTs v1.3.1 emissions product and NIST for funding this project (Project code: 70NANB18H16; Award Number: 70NANB22H219). We thank Kimberly Mueller (NIST) for providing us with model convolutions. Northeast Corridor tower methane observations are available at https://doi.org/10.18434/M32126 (Karion et al., 2019).

Open Research

Methane observations from the Northeast Corridor tower network can be found at https://doi.org/10.18434/M32126 (Karion et al., 2019). STILT model data have been described in Lin et al 2003b (https://doi.org/10.1029/2002JD003161), and the WRF model data have been described in Skamarock et al 2008 (http://dx.doi.org/10.5065/D68S4MVH). The EDGAR 4.2 data have been obtained from http://data.europa.eu/89h/jrc-edgar-emissiontimeseriesv42 and the EDGAR 5.0 have been obtained from http://data.europa.eu/89h/488dc3de-f072-4810-ab83-47185158ce2a. WetCHARTs is described in Bloom et al., (2017).

References

Alvarez, R.A. *et al.* (2012). Greater focus needed on methane leakage from natural gas infrastructure, *Proceedings of the National Academy of Sciences of the United States of America*. *109*(17), pp. 6435–6440. https://doi.org/10.1073/PNAS.1202407109

Alvarez, R.A. *et al.* (2018). Assessment of methane emissions from the U.S. oil and gas supply chain. *Science*, *361*(6398), pp. 186–188. https://doi-org.proxy-um.researchport.umd.edu/10.1126/science.aar7204

Bloom, A. *et al.* (2017). A global wetland methane emissions and uncertainty dataset for atmospheric chemical transport models (WetCHARTs version 1.0). *Geoscientific Model Development*, *10*(6), pp. 2141–2156. https://doi.org/10.5194/GMD-10-2141-2017

Bloomer, B.J., Vinnikov, K.Y. and Dickerson, R.R. (2010). Changes in seasonal and diurnal cycles of ozone and temperature in the eastern U.S. *Atmospheric Environment*, *44*(21–22), pp. 2543–2551. https://doi.org/10.1016/J.ATMOSENV.2010.04.031

Cambaliza, M.O.L. *et al.* (2015). Quantification and source apportionment of the methane emission flux from the city of Indianapolis. *Elementa*, 3. https://doi.org/10.12952/JOURNAL.ELEMENTA.000037

Crippa, M. *et al.* (2019). EDGAR v5.0 Greenhouse Gas Emissions. European Commission, Joint Research Centre (JRC) [Dataset] PID: http://data.europa.eu/89h/488dc3de-f072-4810-ab83-47185158ce2a

Dyer, A.J. (1974). A review of flux-profile relationships," *Boundary-Layer Meteorology 1974 7:3*, *7*(3), pp. 363–372. https://doi.org/10.1007/BF00240838

EDGAR - The Emissions Database for Global Atmospheric Research. https://edgar.jrc.ec.europa.eu/index.php/dataset_ghg50 (Accessed: May 15, 2022).

Gallagher, M.E. *et al.* (2015). Natural Gas Pipeline Replacement Programs Reduce Methane Leaks and Improve Consumer Safety. *Environmental Science & Technology Letters*, *2*(10), pp. 286–291. https://doi.org/10.1021/acs.estlett.5b00213

He, L. *et al.* (2019). Atmospheric Methane Emissions Correlate with Natural Gas Consumption from Residential and Commercial Sectors in Los Angeles. *Geophysical Research Letters*, *46*(14), pp. 8563–8571. https://doi.org/10.1029/2019GL083400

Hendrick, M.F. *et al.* (2016). Fugitive methane emissions from leak-prone natural gas distribution infrastructure in urban environments. *Environmental Pollution*, 213, pp. 710–716. https://doi.org/10.1016/J.ENVPOL.2016.01.094

Horst, T.W. (1999). The footprint for estimation of atmosphere-surface exchange fluxes by profile techniques. *Boundary-Layer Meteorology*, *90*(2), pp. 171–188. https://doi.org/10.1023/A:1001774726067

Huang, Y. *et al.* (2019). Seasonally Resolved Excess Urban Methane Emissions from the Baltimore/Washington, DC Metropolitan Region. *Environmental Science and Technology*, *53*(19), pp. 11285–11293. https://doi.org/10.1021/acs.est.9b02782

Inventory of U.S. Greenhouse Gas Emissions and Sinks | US EPA. https://www.epa.gov/ghgemissions/inventory-us-greenhouse-gas-emissions-and-sinks (Accessed: March 28, 2022).

Jackson, R.B. *et al.* (2014). Natural gas pipeline leaks across Washington, DC. *Environmental Science and Technology*, *48*(3), pp. 2051–2058. https://doi.org/10.1021/ES404474X/ASSET/IMAGES/ES404474X.SOCIAL.JPEG_V03

Janssens-Maenhout, G. *et al.* (2011). Emissions Database for Global Atmospheric Research, version v4.2 (time-series). European Commission, Joint Research Centre (JRC) [Dataset] PID: http://data.europa.eu/89h/jrc-edgar-emissiontimeseriesv42

Janssens-Maenhout, G. *et al.* (2013). Global emission inventories in the Emission Database for Global Atmospheric Research (EDGAR)–Manual (I). *publications.jrc.ec.europa.eu*. https://doi.org/10.2788/81454

Joint Research Centre Data Catalogue - EDGAR v5.0 Greenhouse Gas Emissions - European Commission. https://data.jrc.ec.europa.eu/dataset/488dc3de-f072-4810-ab83-47185158ce2a (Accessed: May 15, 2022).

Karion, A. *et al.* (2019). Observations of CO2, CH4, and CO mole fractions from the NIST Northeast Corridor urban testbed. https://doi.org/10.18434/M32126

Karion, A. *et al.* (2020). Greenhouse gas observations from the Northeast Corridor tower network. *Earth System Science Data*, *12*(1), pp. 699–717. https://doi.org/10.5194/ESSD-12-699-2020

Lamb, B.K. *et al.* (2015). Direct measurements show decreasing methane emissions from natural gas local distribution systems in the United States. *Environmental Science and Technology*, *49*(8), pp. 5161–5169. https://doi.org/10.1021/es505116p

Lamb, B.K. *et al.* (2016). Direct and Indirect Measurements and Modeling of Methane Emissions in Indianapolis, Indiana. *Environmental Science and Technology*, *50*(16), pp. 8910–8917. https://doi.org/10.1021/acs.est.6b01198

Lin, J.C. *et al.* (2003a). A near-field tool for simulating the upstream influence of atmospheric observations: The Stochastic Time-Inverted Lagrangian Transport (STILT) model. *Journal of Geophysical Research: Atmospheres*, *108*(D16), p. 4493. https://doi.org/10.1029/2002JD003161

Lin, J.C. *et al.* (2003b). A near-field tool for simulating the upstream influence of atmospheric observations: The Stochastic Time-Inverted Lagrangian Transport (STILT) model. *Journal of Geophysical Research: Atmospheres*, *108*(D16), p. 4493. https://doi.org/10.1029/2002JD003161

Lopez-Coto, I. *et al.* (2017). Tower-based greenhouse gas measurement network design—The National Institute of Standards and Technology Northeast Corridor Testbed. *Advances in Atmospheric Sciences 2017 34:9*, *34*(9), pp. 1095–1105. https://doi.org/10.1007/S00376-017-6094-6

Lopez-Coto, I. *et al.* (2020). Wintertime CO2, CH4, and CO Emissions Estimation for the Washington, DC–Baltimore Metropolitan Area Using an Inverse Modeling Technique. *Environmental Science & Technology*, *54*(5), 2606–2614. https://doi.org/10.1021/acs.est.9b06619

McKain, K. *et al.* (2015). Methane emissions from natural gas infrastructure and use in the urban region of Boston, Massachusetts. *Proceedings of the National Academy of Sciences of the United States of America*, *112*(7), pp. 1941–1946. https://doi.org/10.1073/PNAS.1416261112

Monteiro, V. *et al.* (2022). The impact of the COVID-19 lockdown on greenhouse gases: a multi-city analysis of in situ atmospheric observations. *Environmental Research Communications*, *4*(4), p. 041004. https://doi.org/10.1088/2515-7620/AC66CB

Mueller, K. *et al.* (2018). Siting Background Towers to Characterize Incoming Air for Urban Greenhouse Gas Estimation: A Case Study in the Washington, DC/Baltimore Area. *Journal of Geophysical Research: Atmospheres*, *123*(5), pp. 2910–2926. https://doi.org/10.1002/2017JD027364

Nehrkorn, T. *et al.* (2010). Coupled weather research and forecasting–stochastic time-inverted Lagrangian transport (WRF–STILT) model. *Meteorology and Atmospheric Physics 2010 107:1*, *107*(1), pp. 51–64. https://doi.org/10.1007/S00703-010-0068-X

Pak, N. *et al.* (2021). The Facility Level and Area Methane Emissions inventory for the Greater Toronto Area (FLAME-GTA). *Atmospheric Environment*, 252, p. 118319. https://doi.org/10.1016/J.ATMOSENV.2021.118319

Patton, E.G., Sullivan, P.P. and Davis, K.J. (2003). The influence of a forest canopy on top-down and bottom-up diffusion in the planetary boundary layer. *Quarterly Journal of the Royal Meteorological Society*, *129*(590), pp. 1415–1434. https://doi.org/10.1256/QJ.01.175

Peischl, J. *et al.* (2013). Quantifying sources of methane using light alkanes in the Los Angeles basin, California. *Journal of Geophysical Research: Atmospheres*, *118*(10), pp. 4974–4990. https://doi.org/10.1002/JGRD.50413

Phillips, N.G. *et al.* (2013). Mapping urban pipeline leaks: Methane leaks across Boston,. *Environmental Pollution*, 173, pp. 1–4. https://doi.org/10.1016/J.ENVPOL.2012.11.003
Plant, G. *et al.* (2019). Large Fugitive Methane Emissions from Urban Centers Along the U.S. East Coast. *Geophysical Research Letters*, *46*(14), pp. 8500–8507. https://doi.org/10.1029/2019GL082635
Ren, X. *et al.* (2018). Methane Emissions from the Baltimore-Washington Area Based on Airborne Observations: Comparison to Emissions Inventories. *Journal of Geophysical Research: Atmospheres*, *123*(16), pp. 8869–8882. https://doi.org/10.1029/2018JD028851
Sargent, M.R. *et al.* (2021). Majority of US urban natural gas emissions unaccounted for in inventories. *Proceedings of the National Academy of Sciences of the United States of America*, *118*(44). https://doi.org/10.1073/pnas.2105804118
Sixth Assessment Report — IPCC. https://www.ipcc.ch/assessment-report/ar6/ (Accessed: August 19, 2022).
Skamarock, W.C. *et al.* (2008). A description of the Advanced Research WRF version 3. NCAR Technical note - 475+STR. http://130.203.136.95/viewdoc/summary?doi=10.1.1.484.3656 (Accessed: July 30, 2022).
Skamarock, W.C. and Klemp, J.B. (2008). A time-split nonhydrostatic atmospheric model for weather research and forecasting applications. *Journal of Computational Physics*, *227*(7), pp. 3465–3485. https://doi.org/10.1016/J.JCP.2007.01.037
Turner, A.J. *et al.* (2016). A large increase in U.S. methane emissions over the past decade inferred from satellite data and surface observations. *Geophysical Research Letters*, *43*(5), pp. 2218–2224. https://doi.org/10.1002/2016GL067987
U.S. Census Bureau QuickFacts: United States. https://www.census.gov/quickfacts/fact/table/arlingtoncountyvirginia,baltimorecitymaryland/SEX255221 (Accessed: November 29, 2022).
Verhulst, K.R. *et al.* (2017). Carbon dioxide and methane measurements from the Los Angeles Megacity Carbon Project - Part 1: Calibration, urban enhancements, and uncertainty estimates. *Atmospheric Chemistry and Physics*, *17*(13), pp. 8313–8341. https://doi.org/10.5194/ACP-17-8313-2017
Weil, J. C., & Horst, T. W. (1992). Footprint estimates for atmospheric flux measurements in the convective boundary layer. *Precipitation Scavenging and Atmosphere-Surface Exchange*, *2*, 717-728.
Weller, Z.D. *et al.* (2022). Environmental Injustices of Leaks from Urban Natural Gas Distribution Systems: Patterns among and within 13 U.S. Metro Areas. *Environmental Science & Technology*, *56* (12), 8599-8609. https://doi.org/10.1021/acs.est.2c00097
Weller, Z.D., Hamburg, S.P. and von Fischer, J.C. (2020). A National Estimate of Methane Leakage from Pipeline Mains in Natural Gas Local Distribution Systems. *Environmental Science and Technology*, *54*(14), pp. 8958–8967. https://doi.org/10.1021/acs.est.0c00437 https://doi.org/10.1021/ACS.EST.0C00437/ASSET/IMAGES/LARGE/ES0C00437_0006.JPEG.
Welp, L.R. *et al.* (2013). Design and performance of a Nafion dryer for continuous operation at CO2and CH4 air monitoring sites. *Atmospheric Measurement Techniques*, *6*(5), pp. 1217–1226. https://doi.org/10.5194/AMT-6-1217-2013
Wunch, D. *et al.* (2009). Emissions of greenhouse gases from a North American megacity. *Geophysical Research Letters*, *36*(15). https://doi.org/10.1029/2009GL039825
Wyngaard, J.C. and Brost, R.A., 1984. Top-down and bottom-up diffusion of a scalar in the convective boundary layer. *Journal of Atmospheric Sciences*, *41*(1), pp.102-112. https://doi.org/10.1175/1520-0469(1984)041%3C0102:TDABUD%3E2.0.CO;2
Yadav, V. et al. (2019). Spatio-temporally Resolved Methane Fluxes from the Los Angeles Megacity. *Journal of Geophysical Research: Atmospheres*, 124(9), pp. 5131–5148. https://doi.org/10.1029/2018JD030062
Yang, L. *et al.* (2018). A new generation of the United States National Land Cover Database: Requirements, research priorities, design, and implementation strategies. *ISPRS Journal of Photogrammetry and Remote Sensing*, 146, pp. 108–123. https://doi.org/10.1016/J.ISPRSJPRS.2018.09.006
Zimmerle, D.J. *et al.* (2015). Methane Emissions from the Natural Gas Transmission and Storage System in the United States. *Environmental Science and Technology*, *49*(15), pp. 9374–9383. https://doi.org/10.1021/acs.est.5b01669